Revista Brasileira de Física, Vol. 3, N.° 3, 1973

The Analog Resonance of ^{208}Pb

JOSÉ ROBERTO BRINATI* and GERHARD W. BUND
Instituto de Fisica Teórica', São Paulo SP

Recebido em 10 de Agosto de 1973

Elastic and inelastic partial proton widths and Coulomb displacement energies for the IAR of the Ground State of ^{208}Pb are calculated in the Blair-Bund model. Exchange terms are included and different optical potentials are considered. Comparison with the experimental widths is made taking into account the off-resonance cross sections predicted by the optical potentials.

Larguras parciais de protons e energias de deslocamento coulombiano são calculadas para a ressonância isobárica análoga ao estado fundamental do ^{208}Pb, a partir do modelo de Blair-Bund. Termos de troca são incluídos nas expressões das larguras parciais e nas energias de deslocamento coulombiano. As larguras parciais são calculadas para diferentes potenciais ópticos e comparadas com resultados experimentais, levando-se em consideração o espalhamento elástico fora da ressonância.

1. Introduction

The analog resonance of the ground state of ^{208}Pb, occuring at 11.50 MeV proton energy, was studied experimentally by several authors[1-4], who obtained its total width and partial elastic and inelastic widths with reasonable accuracy. Theoretically, some calculations have been made[5-8] trying to fit these parameters, within the framework of different models.

Since ^{208}Pb, in its ground state, is a doubly closed shell nucleus, we assume a single particle model representation for the latter, and also for the target and residual nuclei of the elastic and inelastic proton channels, which arise from proton scattering on ^{207}Pb. The states of the residual nuclei are thus described in terms of single neutron-hole states in the excess neutron shells of the ground state of ^{208}Pb. These are, in the order of increasing separation energy, known to be the $3p_{1/2}$, $2f_{5/2}$, $3p_{3/2}$, $1i_{13/2}$, $2f_{7/2}$ and the $1h_{9/2}$ levels.

*Work supported in part by the *Fundação de Amparo à Pesquisa do Estado de São Paulo* (FAPESP).
'Postal address: Caixa Postal 5956, 01000 – S. Paulo SP.

In this paper, we present results in which we try to improve our previous calculations, the basic model[5-7], however, has been kept unaltered, so that no derivation of the relevant formulas will be presented. In this model, a trial wave-function is introduced containing explicitly the analog state and the proton channels. However, orthogonality between these channels and the analog state is not imposed. This approach to analog resonances leads to appreciable simplifications, since antianalog states[8] need not explicitly be introduced. Further, in this model, the coupling between the proton channels and the compound states of the system, with normal isobaric spin, is assumed to be taken into account by the phenomenological optical potential acting in the entrance and exit channels. The coupling between the analog state and the compound states with normal isobaric spin and, also, direct coupling between channels are assumed negligible.

In the present article we improve our calculations in several aspects. First, the exchange terms for the partial widths and Coulomb displacement energy are introduced. Secondly, the phenomenological Coulomb potential, which was formerly[6] utilized in the direct part of those quantities, is now replaced by a Coulomb potential calculated through the single particle proton wave functions. The resultant charge distribution is compared with the experimental charge distribution. Finally, one uses improved optical potentials, that is, potentials giving a better fit to the elastic scattering cross sections off-resonance.

In Sec. 2, we give the formulas used in the calculations of the partial widths and Coulomb displacement energies. In Sec. 3, the potentials are described and, in Sec. 4, the results are presented.

2. Resonance Paramaters

Explicit expressions for the escape amplitude and Coulomb displacement energy are obtained by applying Eqs. (3.19) and (2.12) of Ref. 6, respectively. Thus, for the escape amplitude corresponding to the decay of the analog resonance of ^{208}Pb into channel v, with orbital angular momentum l and spin j for the residual nucleus, we get[7]

$$A_{vlj} = [\Gamma_p^{vlj} \exp(i\varphi_{vlj})]^{1/2} = \left[\frac{4\mu}{\hbar^2 k_v}\right]^{1/2} \left[\frac{1}{(2T_o+1)(2j+1)}\right]^{1/2} \times$$

$$\times \sum_m \int d\mathbf{r} \left[w^{\dagger}_{nvljm}(\mathbf{r})\,(\mathscr{V}_c(r) - E - \varepsilon_n)\,\hat{u}^m_{vlj}(\mathbf{r})\right.$$

$$-\sum_{\lambda m_\lambda} \int d\mathbf{r}' w^{\dagger}_{p\lambda l_\lambda j_\lambda m_\lambda}(\mathbf{r}')\, w^{\dagger}_{n\nu l_\nu j m}(\mathbf{r})\, V_c(|\mathbf{r}-\mathbf{r}'|) \times$$
$$\times\, w_{p\lambda l_\lambda j_\lambda m_\lambda}(\mathbf{r})\, \hat{u}^{m}_{\nu l j}(\mathbf{r}')], \qquad (2\text{-}1)$$

where $\Gamma_p^{\nu l j}$ is the partial width and $\varphi_{\nu l j}$ the associated phase. In Eq. *(2-1)*. T_o is the isospin of the target, $w_{n\nu l j m}$ the wave function of the hole in the parent state which describes the residual nucleus in channel ν and $w_{p\lambda l_\lambda j_\lambda m_\lambda}$ are the wave functions of the protons occupying the parent state. Further, in Eq. (2-1), V_c is the two-body Coulomb interaction, ε_n the neutron separation energy from the parent nucleus, E the proton kinetic energy in the entrance channel, and $\mathscr{V}_c$ the Coulomb potential generated by the protons in ^{208}Pb, given by

$$\mathscr{V}_c(r) = \sum_{\lambda m_\lambda} \int d\mathbf{r}'\, w_{p\lambda l_\lambda j_\lambda m_\lambda}(\mathbf{r}')\, V_c(|\mathbf{r}-\mathbf{r}'|)\, w_{p\lambda l_\lambda j_\lambda m_\lambda}(\mathbf{r}'). \qquad (2\text{-}2)$$

Finally, μ is the reduced mass and k_ν the momentum in channel ν. The function $\hat{u}^{m}_{\nu l j}$ in Eq. *(2-1)* is the partial wave scattering solution of the optical potential equation, appropriate to channel ν

$$(K + V_{\text{opt}} - E,)\, \hat{u}^{m}_{\nu l j} = 0, \qquad (2\text{-}3)$$

where K is the kinetic energy operator, E, the proton energy in channel ν and V_{opt}, a spin-dependent spherical complex optical potential (cf. Eqs. **(3.1)-(3.5)** of Ref. **6).**

The direct term in Eq. *(2-1)* is interpreted as giving rise to the decay of the analog state by emission of a proton lying in an orbit corresponding to the excess neutron shells. The exchange term describes the decay of a proton from the closed proton shells, the hole being then filled by a proton from an orbital corresponding to the neutron excess.

For the Coulomb displacement energy[6,7], assuming that the radial wave functions corresponding to protons and neutrons with identical orbital quantum numbers are the same, one obtains the expression

$$\Delta_c = (2T_o + 1)^{-1} \sum_{\nu m_\nu} \sum_{\mu m_\mu} \int d\mathbf{r}' \int d\mathbf{r}\, w^{\dagger}_{p\nu l_\nu j_\nu m_\nu}(\mathbf{r})\, w^{\dagger}_{n\mu l_\mu j_\mu m_\mu}(\mathbf{r}') \times$$
$$\times\, V(|\mathbf{r}-\mathbf{r}'|)\, [w_{n\mu l_\mu j_\mu m_\mu}(\mathbf{r}')\, w_{p\nu l_\nu j_\nu m_\nu}(\mathbf{r}) -$$
$$w_{n\mu l_\mu j_\mu m_\mu}(\mathbf{r})\, w_{p\nu l_\nu j_\nu m_\nu}(\mathbf{r}')], \qquad (2\text{-}4)$$

where, for the protons the summation extends over all the levels occupied in ^{208}Pb, while for the neutrons, it covers only those levels belonging to the neutron excess.

The "experimental" Coulomb displacement energy is obtained ihrough the expression

$$\mathbf{E}, = \mathbf{A}, + \Delta(E_o) - \mathrm{E}, , \tag{2-5}$$

where **E,** is the proton energy at resonance, E, the neutron separation energy from the parent nucleus and $\Delta(E_o)$ the resonance displacement energy defined through **Eq.** (3.13) of Ref. 6. This energy shift arises from the interaction of the analog state with the other compound states and with the open channels.

In what follows, we shall denote by **(A,),,** and **(A,),,,** the Coulomb displacement energies, obtained respectively from Eqs. **(2-4)** and **(2-5).**

3. Potentials

In the calculation of the wave functions of the bound neutrons from the excess neutron levels, as well as for those corresponding to the bound protons and to the protons in the continuum, a Woods-Saxon central potential well and a Thomas spin-orbit potential were utilized. For the protons, a Coulomb potential generated by a uniform charge distribution was added to these potentials. For the protons in the continuum, one has in addition an imaginary surface potential which was selected to be of the derivative Woods-Saxon form.

The potentials employed may be summarized by the following expression:

$$V = - U_o f(R_o, a_o, r)\, U\, f_{so}(R_{so}, a_{so}, r)\, \boldsymbol{l}\cdot\boldsymbol{\sigma} + U_c(R_c, r)\,\Lambda - iW f_i(R_i, a_i, r), \tag{3-1}$$

where 1 is the orbital angular momentum, $\sigma/2$ the spin operator of the nucleon, **A** a projection operator for the proton states, and W is zero for the bound states.

In Eq. (3.1), f, f_{so} and f_i are given respectively by

$$f(R_o, a_o, r) = [\mathrm{I} + \exp\left(\frac{r - R_o}{a_o}\right)]^{-1}, \tag{3-2}$$

$$f_{so}(R_{so}, a_{so}, r) = \frac{2}{r}\frac{d}{dr} f(R_{so}, a_{so}, r), \tag{3-3}$$

$$f_i(R_i, a,, r) = -4a_i \frac{d}{dr} f(R,, a,, r). \tag{3-4}$$

For the Coulomb potential, one has

$$U_c(R_c, r) = \begin{cases} \dfrac{Ze^2}{8\pi\varepsilon_0}\left[3 - \left(\dfrac{r}{R_c}\right)^2\right], & r < R_c, \\ \dfrac{Ze^2}{4\pi\varepsilon_0}\dfrac{1}{r}, & r > R_c. \end{cases} \tag{3-5}$$

The radii introduced above are given by the relationships

$$R_o = r_o A^{1/3},\ R,, = r,, A^{1/3},\ R_c = r_c A^{1/3},\ R_i = r_i A^{1/3}, \tag{3-6}$$

where A is the mass number of the target.

3.1. Description of the Bound Protons and Neutrons

For the bound protons, the potential parameters given by Rost[9], which describe fairly well proton particle and hole states in ^{208}Pb, were utilized; these parameters are presented in Table 1.

The charge distribution generated by the proton wave functions is plotted in Fig. 1 (curve *a)* and has a r.m.s. radius of *5.42* fm[7]. The radius obtained from electron scattering and from the energy levels of mesic atoms is 5.50 fm[11]; curve b of Fig. 1 represents an empirical charge distribution obtained in this fashion[11]. The Coulomb potential obtained from the shell model wave functions, through Eq. (2.2), and that obtained from the charge distribution of Fig. 1, curve b, were found to be very close to each other. This comparison will be carried further in Section 4, where the results for the partial widths obtained by utilizing both charge distributions are given.

The procedure followed in the evaluation of the single particle wave functions of the neutrons, corresponding to the neutron excess shells, was different from that used for the bound protons. For the neutrons one adjusts the central well depth for each energy level, by fitting the corresponding experimental separation energy. The reason in following this latter procedure lies in that one needs to describe the tail of the neutron wave functions as correctly as possible[12].

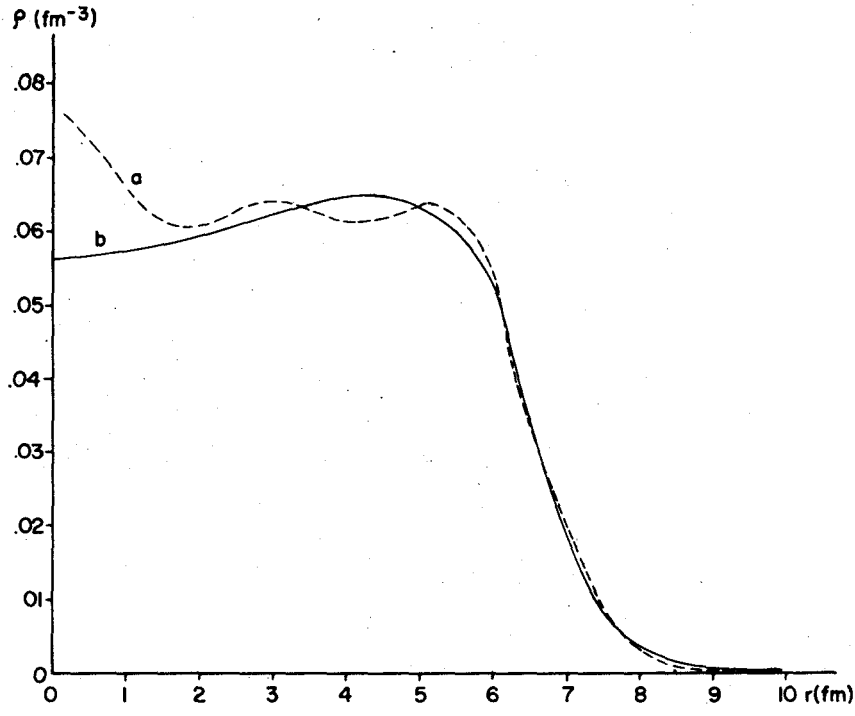

Fig. 1 - a) Charge distribution of ^{208}Pb corresponding to the shell model; b) charge distribution which fits electron scattering and the energy levels of the mesic atoms[11].

For the neutrons, the radius of the central potential as well as the diffuseness were treated, within reasonable limits, as variable parameters. For the spin-orbit potential of the protons as well as of the neutrons, the values r; = 1.01 fm and a„ = 0.75 fm were used For the magnitude of U_{so} we took the value 7.4 MeV for the 3p, 5.0 MeV for the 2f and 6.0 MeV for the 1i and 1h neutron shells.

U_o(MeV)	r_o(fm)	a_o(fm)	U_{so}(MeV)	r_{so}(fm)	a_{so}(fm)	r_c(fm)
60.0	1.26	0.70	5.80	1.01	0.75	1.20

Table 1. Potential parameters for the bound protons in ^{208}Pb.

Potential	U_o (MeV)	r_o (fm)	a_o (fm)	U_{so} (MeV)	r_{so} (fm)	a„ (fm)	W (MeV)	r_i (fm)	a_i (fm)	r_c (fm)
BG	60.9	1.17	0.75	7.4	1.01	0.75	(*)	1.32	0.655	1.20
P	57.1	1.25	0.65	7.4	1.01	0.75	(*)	1.25	0.760	1.25

Table 2. Parameters of the optical potentials; (*) – variable (according to Ref. 13 and Ref. 1, W = 11.4 MeV for BG and $\acute{W}$ = 6.33 MeV for P).

3.2, Description of the Protons in the Continumn

For the description of the proton wave functions in the entrance and exit channels, basically two optical potentials were considered, that of Becchetti and Greenlees[13] (BG), and that of Perey[1] (P), the depth of the imaginary potential being the only parameter which was allowed to vary. We performed an independent fit of the cross sections for proton elastic scattering[1] on ^{207}Pb at 12 MeV in which the imaginary depth W was varied.

In Table 2, the numerical values of the several parameters of these optical potentials are given. In Fig. 2, cross sections for several values of W and the corresponding χ^2 are presented. The values which gave the best fit are W = 6.4 MeV for the potential P with $\chi^2 = 1.4$, and W = 13.0 MeV for BG with $\chi^2 = 7.4$; however W = 10.5 MeV for BG gave also a good fit, with $\chi^2 = 8.0$.

W (MeV)	$(a_o)_n$ (fm)	$(r_o)_n$ (fm)	$\Gamma_p^{1/2}$ (keV)	$\Gamma_p^{5/2}$ (keV)	$\Gamma_p^{3/2}$ (keV)	$\Gamma_p^{7/2}$ (keV)	$(\Delta_c)_{th}$ (MeV)	$(\Delta_c)_{exp}$ (MeV)	$\lvert\xi\rvert$	r_e (fm)	χ^2	β
6.33	0.65	1.11	55.9	27.5	71.2	6.50	19.71	19.66	0.994	5.56	1.4	0.93
7.50	0.65	1.11	51.8	26.1	66.9	6.24	19.71	19.63	1.000	5.56	2.2	0.94
9.00	0.70	1.11	51.4	26.6	67.0	6.44	19.64	19.59	1.029	5.60	4.3	0.95
9.00	0.65	1.13	50.5	26.5	65.9	6.40	19.57	19.58	1.005	5.64	4.3	0.95
10.50	0.65	1.15	48.7	26.5	64.2	6.48	19.43	19.51	1.000	5.71	6.1	0.96
10.50	0.70	1.13	49.6	26.7	65.4	6.53	19.51	19.55	1.024	5.67	6.1	0.96
			56 ± 3	25 ± 3	63 ± 4	4.8 ± 0.8				6.0 ± 0.1		

Table 3. Results for the optical potential P for the proton. W is the depth of the imaginary potential, $(a_o)_n$ and $(r_o)_n$ are respectively the diffuseness and radius of the central neutron potential, Γ_p' is the partial width already multiplied by the correction factor ξ, $(\Delta_c)_{th}$ and $(\Delta_c)_{exp}$ are the theoretical and experimental Coulomb displacement energies, given respectively by Eqs. (2-4) and (2-5); r, is the r.m.s. radius of the neutron excess distribution. Also given are the χ^2 and the normalization factor β corresponding to the fit to the off-resonance scattering cross sections. The last line corresponds to the experimental values for the Γ_p' and r,, given in Refs. 4 and 10, respectively.

4. Results and Conclusions

In order to compare the results from Eq. (2-1), for the partial widths, with those obtained from experiment, one needs to perform corrections arising from the energy dependence of the resonance parameters.

If for the resonance diplacement energy and total width a linear dependente on the energy[6] is assumed, one obtains for the escape amplitude and partial width

$$\tilde{A}_j = \xi^{1/2} A_j , \tag{4-1}$$

$$\tilde{\Gamma}_p^j = |\xi| \Gamma_p^j , \tag{4-2}$$

where the channel independent correction factor 5, given by **Eq. (5.6)** of Ref. **6,** is

$$\xi = [1 - \Delta'(E_o) + \frac{i}{2}\Gamma'(E_o)]^{-1}, \tag{4-3}$$

where A' and Γ' are respectively the derivatives of the resonance displacement energy and total width with respect to the energy. In the evaluation of the latter quantities, **Eq.** (4.12) of Ref. *6* was utilized, with the effective Coulomb potential $\mathscr{V}_c$ given by **Eq. (2-2).**

In what follows, we shall delete the tilde, referring to Γ_p^j and A_j as the energy independent partial widths and escape amplitudes.

W (MeV)	$(a_o)_n$ (fm)	$(r_o)_n$ (fm)	$\Gamma_p^{1/2}$ (keV)	$\Gamma_p^{5/2}$ (keV)	$\Gamma_p^{3/2}$ (keV)	$\Gamma_p^{7/2}$ (keV)	$(\Delta_c)_{th}$ (MeV)	$(\Delta_c)_{exp}$ (MeV)	$\|\xi\|$	r_c (fm)	χ^2	β
6.0	0.70	1.13	52.7	25.3	66.4	5.77	19.51	19.49	0.808	5,67	24.0	0.98
6.0	0.75	1.11	53.8	25.6	67.7	5.82	19.57	19.51	0.826	5.64	24.0	0.98
9.0	0.80	1.13	52.7	27.3	68.0	6.36	19.37	19.47	0.846	5.75	11.0	0.96
9.0	0.85	1.11	53.0	27.1	68.3	6.32	19.42	19.48	0.847	5.72	11.0	0.96
10.5	0.80	1.15	52.5	28.4	68.4	6.70	19.24	19.45	0.863	5.82	8.3	0.95
10.5	0.85	1.13	52.7	28.2	68.6	6.63	19.30	19.46	0.862	5.79	8.3	0.95
11.4	0.75	1.17	49.7	27.6	65.2	6.57	19.17	19.41	0.867	5.86	8.0	0.95
11.4	0.80	1.15	49.9	27.4	65.4	6.50	19.24	19.43	0.868	5.82	8.0	0.95
			56 ± 3	25 ± 3	63 ± 4	4.8 ± 0.8				6.0 ± 0.1		

Tabk 4. Same as Table 3 for optical potential BG.

In Table **3,** we present a summary of our results with potential P, where W takes the values **6.33,** 7.5, **9.0** and **10.5 MeV.** The values for the radius of the neutron central potential (r,), were **1.11, 1.13** and **1.15 fm,** and for the diffusiness ***(a,),*** we took the values **0.65** and **0.70 fm.** For each *W,* we present those cases which give reasonable agreement with the experimental results. In Table 4, similar results are given for the potential BG.

We observe first that the best results for the partial widths were obtained by using the potential **BG** with W = **6.0 MeV;** in the other cases, $\Gamma_p^{7/2}$ is usually appreciably larger than the corresponding experimental value. We also note that the fits to elastic scattering off-resonance for the P-type potentials are better than those obtained through the potentials **BG.**

For the P-type potentials we arrive at the following conclusions: (1) within the theoretical and experimental uncertainties, an acceptable agreement

for the partial widths has been attained for W in the range from 7.5 to 9.0 MeV; (2) for these values of W we have also a good agreement between the Coulomb displacement energies, good values for the χ^2, however the r.m.s. radii r_c of the excess neutron 'distributions fall appreciably below those obtained through other means[10]. It seems however possible to improve somewhat the fit for these radii. For instance, in the case in which $(a_c) = 0.65$ fm and W = 10.5 MeV, by increasing the value of (r_c) to 1.17 fm, the neutron excess r.m.s. radius becomes 5.8 fm, while the values of the partial widths and Coulomb displacement energies are also expected to improve.

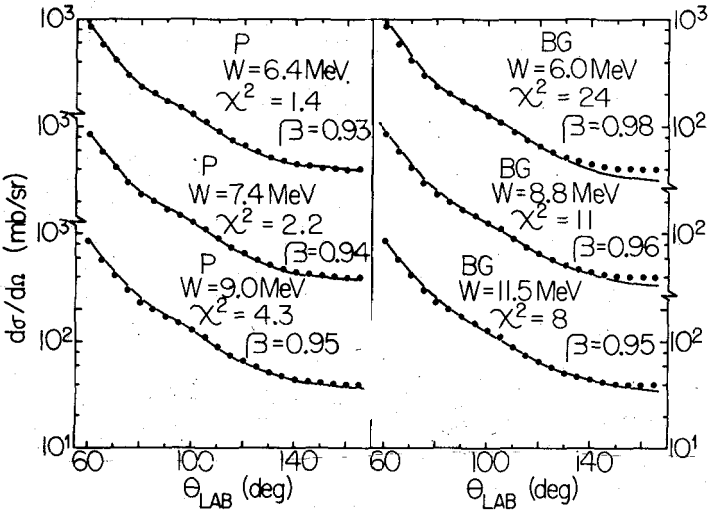

Fig. 2 - Optical model fits for proton elastic scattering on ^{207}Pb at 12 MeV, for P-and BG-type potentials, in which the imaginary depth W is varied. The size of the points indicates statistical uncertainties and β is the normalization constant.

With regard to the BG potentials, we first discuss the results corresponding to values of W between 6.0 and 9.0 MeV, for which the best partial widths have been obtained. In this range of W, we get also reasonable agreement for the Coulomb displacement energies, the best value of χ^2 being reached for W = 9.0 MeV. However, the values of the r.m.s. radii of the excess neutron distributions are still low, although for W = 9.0 MeV they are higher than those discussed previously for the potential P. We remark

here that, for values of W close to 11 MeV for the BG potential, it is still feasible to improve slightly the agreement between the partial widths $\Gamma_p^{1/2}$, the Coulomb displacement energies and the neutron excess r.m.s. radii, by increasing (r,), by about 0.01 fm, at the cost of a slight disagreement for the partial width $\Gamma_p^{5/2}$.

In Table 5, we present the contribution of the exchange part to the escape amplitude for the potential BG with W = 6.0 MeV, (a,), = 0.75 fm and (r,), = 1.11 fm. For these potential parameters, the ratio Δ_c^E/Δ_c^D, of the exchange part to the direct part of the Coulomb displacement energy, was found to be 0.019.

j	$1 + A_j^E/A_j^D$	
	Re.	Im.
1/2	0.9586	+ 0.0001
5/2	0.9539	- 0.0027
3/2	0.9592	- 0.0001
13/2	0.9446	- 0.0045
7/2	0.9582	- 0.0043
9/2	0.9372	- 0.0053

Table 5. Real and imaginary ratios between the total escape amplitudes $A_j + A_j^E$ and direct escape amplitudes A_j^D for potential BG with W = 6.0 MeV, (a,). = 0.75 fm and (r,), = 1.11 fm.

In Table 6, the dependence of the partial widths on the radii (r,), for the neutroncentral potential is studied for a BG – type potential with W = 6.0 MeV and (a), = 0.75 fm. One may observe that the partial widths and the values of $(\Delta_c)_{exp}$ decrease with decreasing (r,), whereas (A,)„ increases.

In Table 7, we show results for the partial widths and Coulomb displacement energies, whose direct part were evaluated by utilizing the Coulomb potential generated by the charge distribution of Fig. 1 (curve b.) For the exchange part of the escape amplitude, the expression

$$A_j^E = A_j^E[A_j^D/A_j^D] \tag{4-4}$$

was used, where A_j^D and A_j^E are, respectively, the direct and exchange amplitudes obtained through the shell model (cf. Eq. (2-I)), and $\bar{A}_j^D$ the direct amplitude obtained through the empirical charge distribution[**]. For the exchange part of the Coulomb displacement energies, an expression analogous to that of Eq. (4.4) was employed.

$\langle r^2 \rangle^{1/2}$ (fm)	I (keV)	$\Gamma_p^{5/2}$ (keV)	$\Gamma^{5/2}_{\gamma}$ (keV)	$\Gamma_p^{1\,3/2}$ (keV)	$\Gamma_p^{7/2}$ (keV)	$\Gamma^{7/2}_{\gamma}$ (keV)	$\lvert\xi\rvert$	$(\Delta_c)_{th}$ (MeV)	$(\Delta_c)_{exp}$ (MeV)
1.15	60.8	29.9	76.4	0.094	6.79	0.020	0.813	19.30	19.54
1.13	57.2	27.6	71.9	0.083	6.28	0.017	0.820	19.43	19.52
1.11	53.8	25.6	67.7	0.074	5.82	0.015	0.826	19.57	19.51

Table 6. Partial widths and Coulomb displacement energies as functions of $\langle r^2 \rangle^{1/2}$; the neutron diffuseness (a) is 0.75 fm. For the protons, the potential is of BG-type with W = 6.0 MeV.

r (fm)	$\Gamma_p^{1/2}$ (keV)	$\Gamma_p^{5/2}$ (keV)	$\Gamma_p^{3/2}$ (keV)	$\Gamma_p^{1\,3/2}$ (keV)	$\Gamma^{3/2}_{\gamma}$ (keV)	$\Gamma^{3/2}_{\gamma}$ (keV)	$\lvert\xi\rvert$	$(\Delta_c)_{th}$ (MeV)	$(\Delta_c)_{exp}$ (MeV)
1.15	60.3	30.1	75.8	0.096	6.62	0.020	0.816	19.29	19.54
1.13	56.5	27.8	71.2	0.084	6.10	0.017	0.820	19.41	19.52
1.11	53.4	25.7	67.3	0.076	5.68	0.015	0.830	19.54	1950

Table 7. Partial widths and Coulomb displacement energies corresponding to the empirical charge distribution of Ref. 11. The potential parameters are identical to those of Table 6.

By comparing Table 6 and Table 7, one notices that the differences between corresponding results of both tables are very small. This fact shows that the resonance parameters are not sensitive to the details of the charge distribution.

The authors are indebted to the staff of the SEMA of the Instituto de Fisica da Universidade de S. Paulo, for the utilization of their computer facilities and for helpful advice in programming. Acknowledgements are also due to Dr. Max Cohenca for putting at our disposal his Computer Program for Optical Model Analysis of Nuclear Scattering.

References

1. D. J. Bredin et al., Phys. Lett. **21,** 677 (1966).
2. B. L. Andersen et al., Phys. Lett. **22,** 651 (1966).
3. G. H. Lenz and G. M. Temmer, Nucl. Phys. **A125** 625 (1968).
4. P. Von Brentano et *al.*, Jahresbericht, Max Planck Institut, Heidelberg (1968).
5. G. W. Bund, Ph. D. Thesis, University of Washington (1968), unpublished.
6. G. W. Bund and J. S. Blair, Nucl. Phys. **A144**, 384 (1970).
7. J. R. Brinati, M. S. Dissertation, University of S. Paulo (1972), unpublished.
8. N. Auerbach et al., Rev. Mod. Phys. 44, 48 (1972).
9. E. Rost, Phys. Lett. **26B**, 184 (1968).
10. H. J. Körner and J. P. Schiffer, Phys. Rev. Lett. **27,** 1457 (1971).
11. H. A. Bethe and L. R. B. Elton, Phys. Rev. Lett. **20**, 745 (1968).
12. R. G. Clarkson et al., Phys. Rev. Lett **26,** 656 (1971).
13. F. D. Becchetti Jr. and G. W. Greenlees, Phys. Rev. **182,** 1190 (1969).